

IR Spectrum of the AsH Radical in its $X^3\Sigma^-$ State, recorded by Laser Magnetic Resonance

Kristine D. Hensel, Rebecca A. Hughes and John M. Brown*

Physical and Theoretical Chemistry Laboratory, South Parks Road, Oxford, UK OX1 3QZ

The IR spectrum of AsH in its ground $^3\Sigma^-$ state has been recorded using CO laser magnetic resonance (LMR). Several molecular parameters of AsH have been determined for the first time. In particular, arsenic nuclear hyperfine structure has been resolved, and the observation of the $v = 2-1$ and $3-2$ hot bands of AsH has allowed an accurate determination of the vibrational anharmonicity, $\omega_e x_e$. Other molecular parameters have been determined more accurately, since Lamb-dip spectra have been recorded, and $\Delta\Omega = \pm 1$ transitions of AsH in its $X^3\Sigma^-$ state have been measured.

The first spectroscopic observation of AsH was by Dixon and co-workers,^{1,2} who studied the $A^3\Pi_1-X^3\Sigma^-$ transition of both AsH and AsD. Nearly 20 years later, the first rotational and vibrational spectra of AsH were recorded, by far-IR LMR³ and IR diode laser spectroscopy,⁴ respectively. More recently, the $b^1\Sigma^+-X^3\Sigma^-$ transition of AsH has been observed.⁵

AsH has also been the subject of several recent theoretical studies;⁶⁻⁹ of particular interest is a comparison of the molecular parameters for the Group 5 (pnictogen) hydrides NH, PH, AsH, SbH and BiH. A notable trend down the group is the increase in the spin-spin splitting in the $X^3\Sigma^-$ ground state: λ_0 grows from 0.91984 cm^{-1} in NH^{10} to 2473.4224 cm^{-1} in BiH^{11} so that while NH and PH follow Hund's case (b) coupling, heavier Group 5 hydrides conform more closely to Hund's case (c). The $\Omega = \pm 1$ spin components of $X^3\Sigma^-$ AsH lie over 100 cm^{-1} above the $\Omega = 0$ component.

The aim of the present work was to record rotation-vibration transitions of AsH using CO LMR in order to improve the precision and accuracy of the known molecular parameters. In particular, it was hoped that $\Delta\Omega \neq 0$ transitions could be recorded, allowing a more direct determination of the spin-spin coupling constant λ than was possible with $\Delta\Omega = 0$ transitions alone.^{3,4} This hope has been realised and, in addition, lines in the $v = 2-1$ and $3-2$ hot bands have been recorded, leading to an accurate determination of the leading term in the vibrational anharmonicity, $\omega_e x_e$.

Experimental

AsH was produced by the reaction between arsenic powder and hydrogen atoms in the intracavity absorption cell of the CO LMR spectrometer; the arrangement of the pumped flow system was very similar to that used to produce TeH in an earlier study.¹³ Hydrogen atoms were produced by a 100 W microwave discharge applied across a mixture of hydrogen and water vapour (200 and 60 mTorr, respectively) flowing through a quartz tube. The products of the discharge were introduced into the cell through a Teflon sleeve directly above the arsenic powder (Aldrich, 99.999+%), which was placed in a porcelain boat on the floor of the cell. The powder was kept level with the rim of the boat and hence below the laser axis. The ends of the cell were purged by helium at a partial pressure of 5 mTorr in order to avoid contamination of the calcium fluoride Brewster windows, although this step was not found to be crucial; the cell was cleaned whenever the arsenic powder was replaced, which was necessary after 4–6 h of experiments.

The CO LMR spectrometer used in this study has been described elsewhere.¹⁴ The CO laser was operated on $\Delta v = 1$ transitions up to the high wavenumber limit (*ca.* 2100 cm^{-1}).

Results and Analysis

LMR Observations

$v = 1-0$ Band

Initial searches for the $v = 1-0$ band of AsH were based on predictions of transition frequencies at zero field, using molecular parameters from ref. 3 and 4. Coincidences were sought on CO laser lines which fell within *ca.* 0.6 cm^{-1} of the predicted transitions, using both parallel ($\Delta M_J = 0$) and perpendicular ($\Delta M_J = \pm 1$) laser polarisations. The signals observed were relatively strong, and many were split into quartets as a result of ^{75}As hyperfine structure ($I_{\text{As}} = 3/2$; ^1H hyperfine structure was not resolved). A representative spectrum is shown in Fig. 1; each M_J component of the $^3P_{22}(4)$ transition† is split into four hyperfine components, which are observed as Lamb dips. In all, six transitions of the $v = 1-0$ band were observed and assigned; these are listed in Table 1, along with the CO laser lines used to record them.

$v = 2-1$ Band

Hot-band transitions of AsH and anticipated coincidences were predicted using the molecular constants of ref. 3 and 4, along with an estimate for $\omega_e x_e$ of 39.4 cm^{-1} , obtained by comparing $\omega_e x_e$ for second- and third-row diatomic hydrides (see below).¹⁵ Transitions of the $v = 2-1$ band of AsH were eventually observed on seven CO laser lines, operating in perpendicular polarisation; these are listed in Table 1. The spectrum observed for the $^3R_{11}(1)$ transition of the $v = 2-1$ band is shown in Fig. 2; note that ^{75}As hyperfine structure has not been resolved for this transition. The present analysis has enabled unassigned lines observed in the diode laser study¹⁶ at 1964.201 and 1950.915 cm^{-1} to be identified respectively as the $^3P_{11}(2)$ and $^3P_{11}(3)$ transitions in the $v = 2-1$ band.

$v = 3-2$ Band

Using the more accurate value of $\omega_e x_e$ which was determined through the observation of $v = 2-1$ transitions, efforts were

† The spin components of the $X^3\Sigma^-$ state of AsH have been labelled F_i in increasing energy order for a given value of J , *i.e.* $F_1 \rightarrow J = N + 1$, $F_2 \rightarrow J = N$, $F_3 \rightarrow J = N - 1$. F_1 corresponds to $\Omega = 0$, while F_2 and F_3 correspond to $\Omega = \pm 1$. Transitions have been labelled to indicate $^N\Delta J_i(N')$, where the transition is from the F_j spin component to the F_i spin component.

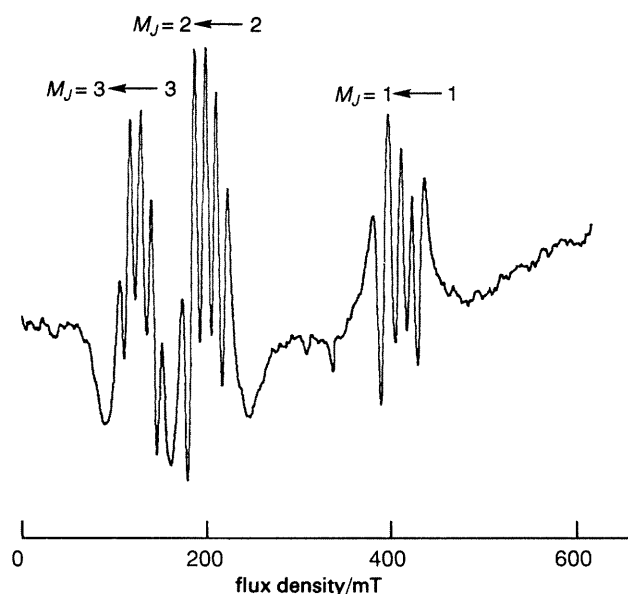


Fig. 1 Portion of the LMR spectrum of the $^{\text{P}}\text{P}_{22}(4)$ transition in the fundamental band of AsH, recorded on the $\text{P}(12)_{4-3}$ laser line ($2016.882\,21\text{ cm}^{-1}$) using parallel polarisation ($\Delta M_J = 0$). Each M_J component is split into a quartet by ^{75}As hyperfine structure, and these quartets are observed as Lamb (saturation) dips burned into the $2-f$ Doppler lineshape. The spectrum was recorded with an output time constant of 300 ms.

also made to locate $v = 3-2$ transitions of AsH. The $^{\text{R}}\text{Q}_{32}(1)$ transition of the $v = 3-2$ band has been observed on the $\text{P}(10)_{8-7}$ CO laser line, but the signals obtained were quite weak. This is consistent with the failure to observe other $v = 3-2$ transitions of AsH: only very weak signals were observed near predicted coincidences, and these could not be assigned to AsH.

Fitting of Data

The data were fitted to an effective Hamiltonian of the form

$$H_{\text{eff}} = H_{\text{ss}} + H_{\text{sr}} + H_{\text{rot}} + H_{\text{cd}} + H_{\text{hfs}} + H_{\text{Q}} + H_{\text{Z}} \quad (1)$$

using Hund's case (a) basis functions. The precise forms of the spin-spin, spin-rotation, rotation, centrifugal distortion, magnetic hyperfine, quadrupole coupling, and Zeeman Ham-

Table 1 Summary of LMR observations of the AsH free radical in the mid-IR

Transition	CO laser line	$\bar{\nu}_{\text{laser}}/\text{cm}^{-1}$
$v = 1 \leftarrow 0$		
$^{\text{P}}\text{Q}_{23}(2)^a$	$\text{P}(11)_{2-1}$	2072.987 97
$^{\text{P}}\text{P}_{22}(4)$	$\text{P}(12)_{4-3}$	2016.882 21
$^{\text{P}}\text{P}_{11}(6)$	$\text{P}(14)_{5-4}$	1982.764 89
$^{\text{P}}\text{Q}_{12}(1)$	$\text{P}(11)_{6-5}$	1969.283 97
$^{\text{P}}\text{Q}_{12}(2)$	$\text{P}(13)_{6-5}$	1961.160 27
$^{\text{N}}\text{P}_{13}(3)$	$\text{P}(8)_{8-7}$	1929.585 71
$v = 2 \leftarrow 1$		
$^{\text{R}}\text{R}_{11}(1)$	$\text{P}(9)_{4-3}$	2029.127 84
$^{\text{R}}\text{R}_{22}(1)$	$\text{P}(10)_{4-3}$	2025.079 44
$^{\text{R}}\text{P}_{13}(1)$	$\text{P}(8)_{5-4}$	2007.145 22
$^{\text{P}}\text{P}_{22}(2)$	$\text{P}(11)_{6-5}$	1969.283 97
$^{\text{P}}\text{P}_{33}(3)$	$\text{P}(6)_{7-6}$	1963.082 82
$^{\text{P}}\text{P}_{11}(5)$	$\text{P}(10)_{8-7}$	1921.802 81
$^{\text{P}}\text{Q}_{12}(1)$	$\text{P}(5)_{10-9}$	1889.466 57
$v = 3 \leftarrow 2$		
$^{\text{R}}\text{Q}_{32}(1)$	$\text{P}(10)_{8-7}$	1921.802 81

^a The value of N'' is given in parentheses.

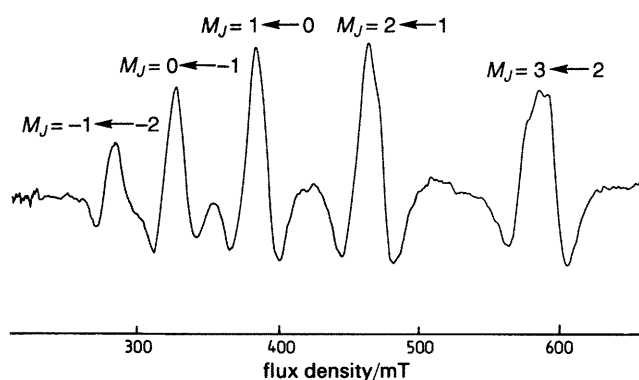


Fig. 2 Portion of the LMR spectrum of the $^{\text{R}}\text{R}_{11}(1)$ transition in the $v = 2-1$ hot band of AsH, recorded on the $\text{P}(9)_{4-3}$ laser line ($2029.127\,84\text{ cm}^{-1}$) using perpendicular polarisation ($\Delta M_J = \pm 1$). The hyperfine structure of this transition has not been resolved. The spectrum was recorded with a time constant of 1 s.

iltonians have been described elsewhere.¹⁷ The vibrational dependence of the parameters of H_{eff} was modelled as¹⁴

$$P_v = P_e + \alpha_P(v + \frac{1}{2}) + \beta_P(v + \frac{1}{2})^2 + \dots \quad (2)$$

so that α_B is opposite in sign to Herzberg's α_e .¹⁸ Three parameters which were indeterminable were constrained in the fit. H_0 was constrained to a value calculated using

$$H_0 \approx H_e = \frac{2}{3}D_e \left\{ 12 \left(\frac{B_e}{\omega_e} \right)^2 + \frac{\alpha_B}{\omega_e} \right\} \quad (3)$$

g_N was set to its known value for atomic As,¹⁹ and g_{r_0} was constrained to the value obtained in the FIR LMR study.³

Measurements from both FIR LMR³ and IR diode laser studies⁴ were included in the data sets for all fits, along with the CO LMR measurements gathered in this work and the two diode laser measurements which have been assigned in the $v = 2-1$ band as a result of the present study. Experimental uncertainties for the FIR LMR and diode laser data were assigned as 3×10^{-5} and $1 \times 10^{-2}\text{ cm}^{-1}$, respectively, although diode laser data which were given zero weight in the fit described in ref. 4 were also given zero weight here. Doppler-limited peaks from the present work were assigned experimental uncertainties of $1 \times 10^{-3}\text{ cm}^{-1}$, while Lamb-dip spectra were assigned a lower uncertainty of $3 \times 10^{-4}\text{ cm}^{-1}$. Initial fits were performed without the $v = 2-1$ and $3-2$ measurements, in order to determine the $v = 0$ and $v = 1$ molecular parameters conclusively before making a final assignment of the hot-band transitions. The parameters obtained from the final fit, including $v = 2-1$ and $3-2$ data, are given in Table 2; a detailed description of the CO LMR data included in the fit is given in Table 3, along with the tuning rates $\partial\nu/\partial B_0$. For the more slowly tuning transitions, it was often not possible to resolve the ^{75}As nuclear hyperfine structure. The absolute standard deviation, σ , for the fit of this data is $9.7 \times 10^{-4}\text{ cm}^{-1}$, while $\sigma = 1.9 \times 10^{-5}\text{ cm}^{-1}$ for the FIR LMR data and $\sigma = 9.7 \times 10^{-3}\text{ cm}^{-1}$ for the diode laser data; these values are consistent with the estimated uncertainties of the data.

Discussion

A schematic diagram of the type of rotational-vibrational transitions measured in the present and other studies is given in Fig. 3. Particularly significant transitions are those which connect spin states with different values of Ω , such as the $^{\text{R}}\text{R}_{13}(1)$ and the $^{\text{P}}\text{Q}_{23}(2)$ transitions; these have been measured for the first time in this work. As a result, the spin-spin coupling constant, λ_0 , and the spin-rotation coupling constant,

Table 2 Molecular parameters determined for ^{75}AsH in the $X^3\Sigma^-$ state

parameter	value ^a	correlation, κ_i ^b
$\tilde{\nu}_0$	2076.925 28 (89)	284.501
$\omega_e x_e$	39.222 72 (87)	148.618
$10^1 \omega_e y_e$	-0.405 8 (13)	99.885
B_0	7.201 133 (16)	414.164
α_B	-0.211 774 (72)	260.724
$10^4 \beta_B$	-0.47 (19)	89.952
$10^3 D_0$	0.334 92 (53)	422.376
$10^5 \alpha_D$	-0.261 (70)	7.104
$10^8 H_0$	0.888 ^c	
λ_0	58.852 5 (10)	464.335
$10^1 \alpha_\lambda$	0.784 (17)	542.778
$10^1 \beta_{\lambda_0}$	-0.210 2 (41)	174.584
$10^3 \lambda_D$	0.168 (41)	2345.017
γ_0	-0.273 37 (24)	3053.239
$10^1 \alpha_\gamma$	0.144 2 (18)	16.282
$10^4 \gamma_D$	0.560 (50)	494.743
$10^2 b$	0.493 7 (27)	1.010
$10^1(b+c)$	-0.110 72 (63)	1.041
$10^3 \alpha_{(b+c)}$	-0.23 (19)	1.075
$10^2 e Q q_0$	-0.319 (13)	1.000
g_{S_0}	2.005 6 (11)	388.285
$10^2 g_{\alpha}$	0.83 (10)	2.353
$10^3 g_{\alpha_0}$	-0.62 ^c	
$10^1 g_i$ ^e	0.107 (12)	313.869
g_N ^d	0.9597 ^c	

^a Values quoted in cm^{-1} , except for g -factors; the numbers in parentheses correspond to one standard deviation of the least-squares fit. ^b Correlation parameter $\kappa_i = (\chi^{-1})_{ii}$ where χ is the matrix of correlation coefficients. ^c Parameter constrained to this value in the fit (see text). ^d Nuclear g -factor for ^{75}As .

γ_0 , have been determined directly, giving more accurate values which differ somewhat from the values determined indirectly from $\Delta\Omega = 0$ transitions alone. Several of the molecular parameters which we have determined are compared with previously determined values in Table 4.

As $v = 2-1$ and $3-2$ transitions of AsH have been observed in this study for the first time, the vibrational dependences of several parameters, including the hyperfine parameter $(b+c)$,

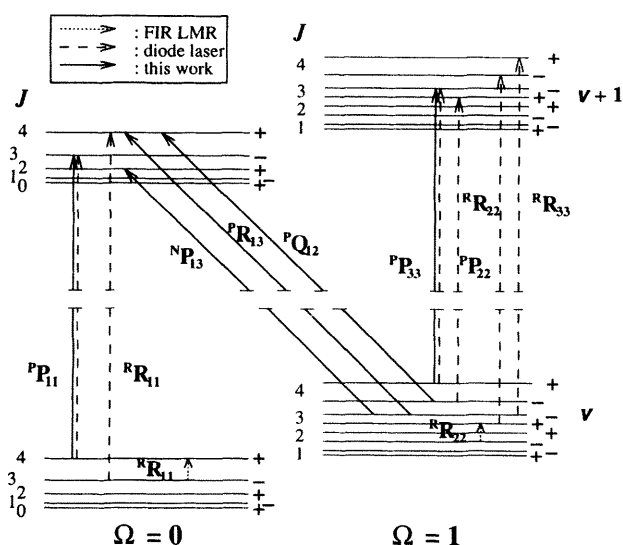


Fig. 3 Schematic energy-level diagram for AsH in the $X^3\Sigma^-$ state, showing the types of transitions which have been measured by FIR LMR,³ IR diode laser,⁴ and CO LMR techniques (this work). The energy levels are labelled by their value of J and their parity.

have been determined. In particular, the vibrational anharmonicity, $\omega_e x_e$, has been measured very accurately; the parameter $\omega_e y_e$ has also been determined, although probably less reliably because of neglect of higher-order terms. In addition, both the precision and the accuracy of the band origin, $\tilde{\nu}_0$, have been improved over the value determined in the diode laser study, as a result of the inherent accuracy and precision of the CO LMR technique. The observation of several Lamb-dip spectra has also contributed to the increased accuracy.

One of the manifestations of Hund's case (c) behaviour for a molecule in a $^3\Sigma$ state is the occurrence of well behaved Ω -type doubling in the $\Omega = 1$ component,²⁰ the splitting increasing as $J(J+1)$. Although this doubling is obvious for the lowest levels of AsH (see Fig. 3), for $J > 5$ the doubling becomes comparable with the spacing between rotational levels and is much more difficult to pick out. This marks the tendency towards Hund's case (b) coupling for these levels.

Comparison with Other Group 5 Hydrides

Values of ω_e and B_e are listed in Table 5 for four Group 5 hydrides. Values of the stretching force constant k ($k = 4\pi^2 c^2 \mu \omega_e^2$, where μ is the reduced mass and c is the speed of light) and the pnictogen-hydrogen bond length r_e have also been calculated and tabulated. As would be expected, the force constant decreases down the group as r_e increases. The bond lengths observed also agree well with the sums of the pnictogen and hydrogen single bond covalent radii.³⁶ Trends in the hyperfine parameters of the Group 5 diatomic hydrides have been discussed in ref. 3.

Vibrational Anharmonicity of Second- and Third-row Diatomic Hydrides

As has been noted previously,¹⁵ trends in the known anharmonicities of diatomic hydrides may be used to estimate $\omega_e x_e$ for other diatomic hydrides. In order to predict zero-field transition wavenumbers for the $v = 2-1$ band of AsH, the values of $\omega_e x_e$ for second-row diatomic hydrides were plotted against $\omega_e x_e$ for third-row diatomic hydrides, which gave an initial estimate of $\omega_e x_e = 39.4 \text{ cm}^{-1}$ for AsH. This plot is reproduced in Fig. 4, using $\omega_e x_e = 39.222 72 \text{ cm}^{-1}$ for AsH, as determined in this study; the periodicity of $\omega_e x_e$ for diatomic hydrides is clearly apparent. The estimate of $\omega_e x_e$

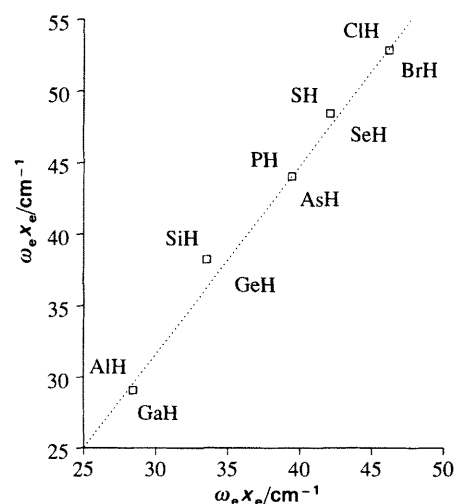


Fig. 4 $\omega_e x_e$ for second-row diatomic hydrides vs. $\omega_e x_e$ for third-row diatomic hydrides. Values of $\omega_e x_e$ are taken from ref. 21 (AlH), 22 (SiH), 32, (PH), 24 (SH), 25 (CIH), 26 (GaH), 27 (GeH), 28 (SeH), scaled from $\omega_e x_e$ for SeD), 29 (BrH), and this work (AsH).

Table 3 Details of the least-squares fit of the AsH data

M_I^a	M_J	M_J''	B_{obs}/mT	$o-c^b$	$(\partial v/\partial B_0)$ (MHz mT ⁻¹)	M_I^a	M_J	M_J''	B_{obs}/mT	$o-c^b$	$(\partial v/\partial B_0)$ (MHz mT ⁻¹)
$v = 1-0$ band						$v = 2-1$ band					
^P Q ₂₃ (2) ^f			$\tilde{\nu}_{\text{laser}} = 2072.98797 \text{ cm}^{-1}$						$\tilde{\nu}_{\text{laser}} = 1929.58571 \text{ cm}^{-1}$		
3/2	1	0	1045.6	-3.6	1.5	-1/2			966.4	-7.8	-10.0
1/2			1033.0	-2.2	1.5	-3/2			978.6	-9.3	-10.0
-1/2			1021.8	-2.5	1.5	^N P ₁₃ (3)	1	2	1124.8	12.8	12.1
-3/2			1010.6	1.5	1.5	3/2			1141.4	9.0	12.1
						1/2			1157.3	9.0	12.1
						-1/2			1173.4	9.7	12.1
^P P ₂₂ (4)			$\tilde{\nu}_{\text{laser}} = 2016.88221 \text{ cm}^{-1}$								
3/2	3	3	153.4	0.9	2.7						
1/2			142.1	1.6	2.7						
-1/2			130.1	1.8	2.7						
-3/2			118.2	2.0	2.8	^R R ₁₁ (1)			$\tilde{\nu}_{\text{laser}} = 2029.12784 \text{ cm}^{-1}$		
3/2	2	2	223.9	0.5	1.8	e	-1	-2	278.8	24.6	7.9
1/2			211.9	1.0	1.8	e	0	-1	322.8	17.2	6.8
-1/2			199.5	1.1	1.8	e	1	0	380.6	11.6	5.8
-3/2			186.5	1.4	1.9	e	2	1	461.2	6.0	4.8
3/2	1	1	433.6	-0.3	0.9	e	3	2	582.0	-1.9	3.9
1/2			422.5	-0.4	0.9	^R R ₂₂ (1)			$\tilde{\nu}_{\text{laser}} = 2025.07944 \text{ cm}^{-1}$		
-1/2			409.6	-0.3	0.9	3/2	0	-1	660.7	-7.7	14.7
-3/2			395.1	0.0	0.9	1/2			648.2	-6.5	14.7
3/2	3	4	294.3	-0.2	1.4	-1/2			636.4	-6.8	14.7
1/2			275.1	1.4	1.4	-3/2			624.4	-4.4	14.7
-1/2			262.3	1.3	1.4	^P R ₁₃ (1)			$\tilde{\nu}_{\text{laser}} = 2007.14522 \text{ cm}^{-1}$		
-3/2			251.8	1.4	1.4	3/2	-2	-1	1150.2	-1.3	7.7
3/2	2	1	141.2	-8.3	3.2	1/2			1165.6	2.8	7.6
1/2			129.3	-5.7	3.2	-1/2			1180.1	8.1	7.6
-1/2			119.3	-7.2	3.2	-3/2			1197.3	5.0	7.6
-3/2			109.7	-10.2	3.3	e	-1	-2	857.2	9.7	10.9
3/2	1	0	177.8	3.0	2.3	^P P ₂₂ (2)			$\tilde{\nu}_{\text{laser}} = 1969.28397 \text{ cm}^{-1}$		
1/2			166.8	3.6	2.3	3/2	-1	0	927.1	3.2	-15.0
-1/2			154.0	4.3	2.3	1/2			914.9	3.2	-14.9
-3/2			141.2	4.2	2.3	-1/2			902.8	2.2	-14.9
3/2	0	-1	294.3 ^d	-1.5	1.4	-3/2			890.7	-0.1	-14.9
1/2			275.1 ^d	2.2	1.4	^P P ₃₃ (3)			$\tilde{\nu}_{\text{laser}} = 1963.08282 \text{ cm}^{-1}$		
-1/2			262.3 ^d	2.6	1.4	e	1	2	1236.9	-7.3	10.7
-3/2			251.8 ^d	1.6	1.4	^P P ₁₁ (5)			$\tilde{\nu}_{\text{laser}} = 1921.80281 \text{ cm}^{-1}$		
						e	-5	-4	445.4 ^d	20.6	-6.5
^P P ₂₂ (4)			$\tilde{\nu}_{\text{laser}} = 2016.88221 \text{ cm}^{-1}$			e	-4	-3	478.6 ^d	13.0	-6.0
3/2	-1	-2	756.3	3.2	0.6	e	-3	-2	515.7	1.5	-5.5
1/2			739.3	3.7	0.6	e	-2	-1	565.3	-1.4	-5.0
-1/2			726.8	4.1	0.6	e	-1	0	626.7	-3.2	-4.5
-3/2			722.6	3.8	0.6	e	0	1	699.0	-10.6	-4.0
3/2	2	3	797.9	-4.1	0.6	e	1	2	794.8	-14.5	-3.5
1/2			776.2	-4.0	0.5	e	2	3	919.3	-21.1	-3.0
-1/2			756.3	-2.7	0.5	e	3	4	1141.5	13.3	-2.5
-3/2			756.3	-3.7	0.5	e	-5	-5	1156.3	15.0	-2.5
^P P ₁₁ (6)			$\tilde{\nu}_{\text{laser}} = 1982.76489 \text{ cm}^{-1}$			^P Q ₁₂ (1)			$\tilde{\nu}_{\text{laser}} = 1889.46657 \text{ cm}^{-1}$		
e	-6	-5	1.8	0.5	-6.1	e	0	1	1452.3	-37.2	-14.2
^P Q ₁₂ (1)			$\tilde{\nu}_{\text{laser}} = 1969.28397 \text{ cm}^{-1}$								
3/2	-1	-1	510.2	3.9	6.1						
1/2			479.6	3.5	6.1						
-1/2			447.7	2.6	6.1						
-3/2			414.4	1.5	6.1						
e	1	0	380.3	-3.2	7.5	^R Q ₃₂ (1)			$\tilde{\nu}_{\text{laser}} = 1921.80281 \text{ cm}^{-1}$		
3/2	0	-1	222.0	6.1	14.0	3/2	0	1	229.2	14.8	-1.4
1/2			208.7	6.1	14.0	1/2			214.2	-2.7	-1.4
-1/2			197.1	5.6	14.0	-1/2			200.2	-20.0	-1.4
-3/2			186.2	10.2	14.0	-3/2			186.9	-37.5	-1.4
^P Q ₁₂ (2)			$\tilde{\nu}_{\text{laser}} = 1961.16027 \text{ cm}^{-1}$			3/2	-1	0	478.6 ^d	32.2	-0.7
e	-1	0	1212.5	-6.6	-8.3	1/2			445.4 ^d	19.8	-0.7
3/2	-2	-1	945.7	-8.5	-10.0	-1/2			413.2	19.2	-0.7
1/2			955.1	-8.7	-10.0	-3/2			391.5	22.0	-0.7
						e	1	1	410.4	4.2	-0.7

^a $\Delta M_I = 0$. ^b $(\tilde{\nu}_{\text{laser}} - \tilde{\nu}_{\text{calc}})/10^{-4} \text{ cm}^{-1}$. ^c The value of N'' is given in parentheses. ^d Resonance given zero weight in the fit. ^e Hyperfine structure not resolved in observed spectra.

Table 4 Comparison of selected present and previously determined parameters for ^{75}AsH in the $X^3\Sigma^-$ state

parameter ^a	previous ^b	present
$\tilde{\nu}_0$	2076.874 (28)	2076.925 28 (89)
$\omega_e x_e$	49 ^c	39.222 72 (87)
B_0	7.200 899 6 (77)	7.201 133 (16)
α_B	-0.211 72 (99)	-0.211 774 (72)
$10^3 D_0$	0.328 0 (37)	0.334 92 (53)
λ_0	58.823 6 (19)	58.852 5 (10)
γ_0	-0.270 67 (20)	-0.273 37 (24)
g_{S_0}	1.997 2 (33)	2.005 6 (11)

^a Values quoted in cm^{-1} , except for g -factors; the numbers in parentheses correspond to three standard deviations of the least-squares fit. ^b Ref. 3 and 4. ^c Estimated in ref. 4.

obtained in this manner turned out to be surprisingly accurate compared with the estimate of $\omega_e x_e = 49 \text{ cm}^{-1}$ given in ref. 4, and assignment of the $v = 2-1$ and $3-2$ band observations was simplified considerably as a result.

Interpretation of Electron Spin Parameters

Spin-Rotation Coupling

The spin-rotation parameter, γ , arises predominantly from the spin-orbit mixing of the $^3\Sigma^-$ ground state of AsH with low-lying $^3\Pi$ states. This second-order contribution is given

by³⁷

$$\gamma^{(2)} = -2 \sum_n \frac{\langle 0 | BL_+ | n \rangle \langle n | AL_- | 0 \rangle}{E_0 - E_n} \quad (4)$$

where the summation is over all vibronic states $|n\rangle$ other than the vibronic state of interest ($n = 0$). If the lowest excited $^3\Pi$ state of AsH, which lies $29\,880.65 \text{ cm}^{-1}$ above the ground state,² is considered to be formed by the promotion of an electron from a molecular orbital resembling an As $4p_\sigma$ atomic orbital (AO) to one resembling an As $4p_\pi$ AO, then $\gamma^{(2)}$ may be approximated as

$$\gamma^{(2)} = \frac{2BA}{E_{3\Pi} - E_{3\Sigma^-}} \quad (5)$$

Using the rotational constant determined in this work and the spin-orbit coupling constant $A = -615.35 \text{ cm}^{-1}$,² the spin-rotation coupling constant is calculated from eqn. (5) as $\gamma^{(2)} = -0.2966 \text{ cm}^{-1}$; this value compares very well with $\gamma_0 = -0.273\,37 \text{ cm}^{-1}$, as determined in this study.

Spin-Spin Coupling

The predominant contribution to the spin-spin coupling constant, λ , for AsH is the result of a second-order spin-orbit interaction of the $X^3\Sigma^-$ ground state with the $^1\Sigma_g^+$ state arising from the same $\sigma^2\pi^2$ electronic configuration.² In these

Table 5 Comparison of molecular parameters for Group 5 hydrides

parameter	$^{14}\text{NH}^a$	$^{31}\text{PH}^b$	$^{75}\text{AsH}^c$	$^{121}\text{SbH}^d$	$^{209}\text{BiH}^e$
ω_e/cm^{-1}	3282.583	2363.779	2155.503	1896.760	1697.6278
k/Nm^{-1}	596.87	321.32	272.23	211.86	170.31
B_e/cm^{-1}	16.6670	8.5390	7.3070	5.7627	5.1378
$r_e/\text{\AA}$	1.0372	1.4222	1.5231	1.7108	1.8087
$r_{\text{pred}}^f/\text{\AA}$	1.03	1.40	1.51	1.71	

^a Ref. 30, 31, and 10. ^b Ref. 32 and 33. ^c This work. ^d Ref. 34. ^e Ref. 35. Note that these parameters correspond to the $X0^+$ state of BiH only. ^f Bond length predicted using the single bond covalent radii given in ref. 36.

Table 6 Calculated wavenumbers of the mid-IR spectrum of ^{75}AsH in its $X^3\Sigma^-$ state: $\Delta\Omega = 0$ transitions

N''	$^{\text{P}}P_{11}$	$^{\text{P}}P_{22}$	$^{\text{P}}P_{33}$	$^{\text{R}}R_{11}$	$^{\text{R}}R_{22}$	$^{\text{R}}R_{33}$
$v = 1 \leftarrow 0$						
0				2097.320		
1	2054.731 ^a			2108.636	2104.458	2197.716
2	2042.178	2047.717	1954.974	2120.316	2117.564	2111.067
3	2028.507	2032.493	2040.211	2132.070	2130.223	2125.954
4	2013.936	2016.869	2022.325	2143.689	2142.426	2139.582
5	1998.648	2000.854	2004.758	2155.044	2154.167	2152.226
6	1982.765	1984.456	1987.308	2166.053	2165.437	2164.079
7	1966.369	1967.683	1969.810	2176.664	2176.229	2175.256
8	1949.512	1950.544	1952.156	2186.845	2186.536	2185.823
9	1932.232	1933.046	1934.284	2196.569	2196.351	2195.817
10	1914.557	1915.199	1916.154	2205.821	2205.667	2205.258
$v = 2 \leftarrow 1$						
0				2018.099		
1	1976.408			2029.052	2024.771	2118.729
2	1964.194	1969.726	1876.378	2040.323	2037.453	2030.999
3	1950.915	1954.925	1962.635	2051.649	2049.688	2045.400
4	1936.760	1939.734	1945.256	2062.837	2061.467	2058.590
5	1921.897	1924.131	1928.143	2073.759	2072.784	2070.813
6	1906.441	1908.155	1911.121	2084.337	2083.630	2082.250
7	1890.472	1891.803	1894.042	2094.519	2094.000	2093.012
8	1874.041	1875.084	1876.804	2104.271	2103.883	2103.163
9	1857.186	1958.007	1859.345	2113.569	2113.275	2112.740
10	1839.934	1840.578	1841.630	2122.395	2122.167	2121.764

^a Calculated zero-field wavenumber/ cm^{-1} .

Table 7 Calculated wavenumbers of the mid-IR spectrum of ^{75}AsH in its $X^3\Sigma^-$ state: $\Delta\Omega = \pm 1$ transitions^a

N''	$^PQ_{12}$	$^PQ_{23}$	$^PR_{13}$	$^RQ_{21}$	$^RQ_{32}$	$^RP_{31}$	$^NP_{13}$	$^TP_{31}$
$v = 1 \leftarrow 0$								
0				2183.570		2066.051		2222.144
1	1969.188 ^b		2086.620	2190.002	2080.284	2165.828		2251.570
2	1961.467	2072.493	1986.242	2198.276	2086.292	2167.003		2284.260
3	1951.127	2064.385	1983.020	2207.602	2094.061	2171.441	1929.115	2318.909
4	1938.909	2053.597	1975.638	2217.453	2102.854	2177.881	1897.500	2354.652
5	1925.321	2040.919	1965.387	2227.493	2112.161	2185.488	1861.824	2390.934
$v = 2 \leftarrow 1$								
0				2104.996		1987.474		2142.095
1	1890.157		2007.677	2111.022	2001.210	2087.460		2170.225
2	1882.828	1993.900	1907.002	2118.819	2006.825	2088.191		2201.524
3	1872.955	1986.197	1904.227	2127.648	2014.128	2092.088	1851.583	2234.757
4	1861.227	1975.885	1897.389	2137.000	2022.428	2097.961	1821.260	2269.090
5	1848.134	1963.703	1887.705	2146.548	2031.241	2105.005	1786.970	2303.975

^a Strictly speaking, the $^PQ_{23}$ and $^RQ_{32}$ branches are $\Delta\Omega = 0$ transitions. ^b Calculated zero-field wavenumber/cm⁻¹.

circumstances, $\lambda^{(2)}$ is given by

$$\lambda^{(2)} = \frac{-2A^2}{E_{3\Sigma^-} - E_{1\Sigma^+}} \quad (6)$$

Given the spin-orbit coupling constant determined in ref. 2 and $T_e(b^1\Sigma^+ - X^3\Sigma^-) = 14\,178.0 \text{ cm}^{-1}$ from ref. 5, $\lambda^{(2)} = 53.41 \text{ cm}^{-1}$, which is reasonably close to the value of $\lambda_0 (= 58.8531 \text{ cm}^{-1})$ determined here.

Future Work

As the CO laser is not continuously tunable, many rotational-vibrational transitions of AsH could not be observed in this study. The parameter values in Table 2 have been used to make predictions of zero-field $\Delta\Omega = 0$ transition wavenumbers in the mid-IR which are listed in Table 6; predictions of $\Delta\Omega = \pm 1$ transitions are given in Table 7. Although the latter transitions are much weaker than the main P- and R-branch transitions, some of them have been detected in the present work, a tribute to the sensitivity of the LMR technique.

During the course of this work, resonances which did not correspond to any AsH transitions were observed on several of the CO laser lines which were scanned. As some of these resonances displayed closely spaced quartet structure and as AsH₂ is likely to be present in the discharge plasma, it is hoped that they are the result of rotational-vibrational transitions in either the symmetric or asymmetric stretching fundamental bands of AsH₂, about which nothing is currently known. Laser lines near the high-wavenumber limit of the CO laser are currently being scanned in a search for further coincidences.

We are very grateful to Dr. David A. Gillett for his assistance with the CO laser, and to Dr. Richard Barrow for a critical reading of the manuscript. K.D.H. thanks the Natural Sciences and Engineering Research Council of Canada for a Postdoctoral Fellowship.

References

- R. N. Dixon, G. Duxbury and H. M. Lamberton, *Chem. Commun.*, 1966, 460.
- R. N. Dixon and H. M. Lamberton, *J. Mol. Spectrosc.*, 1968, **25**, 12.
- K. Kawaguchi and E. Hirota, *J. Mol. Spectrosc.*, 1984, **106**, 423.
- J. R. Anacona, P. B. Davies and S. A. Johnson, *Mol. Phys.*, 1985, **56**, 989.
- M. Arens and W. Richter, *J. Chem. Phys.*, 1990, **93**, 7094.
- L. G. M. Pettersson and S. R. Langhoff, *J. Chem. Phys.*, 1986, **85**, 3130.
- T. Matsushita, C. M. Marian, R. Klotz and S. D. Peyerimhoff, *Can. J. Phys.*, 1987, **65**, 155.
- K. Balasubramanian and V. Nannegari, *J. Mol. Spectrosc.*, 1989, **138**, 482.
- M. Kloubkowski, *Chem. Phys. Lett.*, 1991, **183**, 417.
- D. Boudjaadar, J. Brion, P. Chollet, G. Guelachvili and M. Vervloet, *J. Mol. Spectrosc.*, 1986, **119**, 352.
- E. H. Fink, K. D. Setzer, D. A. Ramsay, M. Vervloet and J. M. Brown, *J. Mol. Spectrosc.*, 1990, **142**, 108.
- V. Stackmann, K. Lipus and W. Urban, *Mol. Phys.*, 1993, **80**, 635.
- D. A. Gillett, J. P. Towle, M. Islam and J. M. Brown, *J. Mol. Spectrosc.*, 1994, **163**, 459.
- J. P. Towle and J. M. Brown, *Mol. Phys.*, 1993, **78**, 249.
- A. D. Fackerell, Ph.D. Thesis, Southampton University, 1981.
- S. A. Johnson, Ph.D. Thesis, Cambridge University, 1986.
- J. M. Brown, I. Kopp, C. Malmberg and B. Rydh, *Phys. Scr.*, 1978, **17**, 55.
- G. Herzberg, *Molecular Spectra and Molecular Structure, Vol. I, Spectra of Diatomic Molecules*, Krieger, Malabar, FL, 2nd edn. (corrected), 1989.
- International Union of Pure and Applied Chemistry, *Quantities, Units, and Symbols in Physical Chemistry*, ed. I. Mills, T. Cvitaš, K. Homann, N. Kallay and K. Kuhitsu, Blackwell Scientific, Oxford, 2nd edn., 1993.
- L. Veseth, *J. Phys. B*, 1973, **6**, 1473.
- C. Yamada and E. Hirota, *Chem. Phys. Lett.*, 1992, **197**, 461.
- W. Seebass, J. Werner, W. Urban, E. R. Comben and J. M. Brown, *Mol. Phys.*, 1987, **62**, 161.
- R. S. Ram and P. F. Bernath, *J. Mol. Spectrosc.*, 1987, **122**, 275.
- P. F. Bernath, T. Amano and M. Wong, *J. Mol. Spectrosc.*, 1983, **98**, 20.
- D. H. Rank, B. S. Rao and T. A. Wiggins, *J. Mol. Spectrosc.*, 1965, **17**, 122.
- J. M. Campbell, M. Dulick, D. Klapstein, J. B. White and P. F. Bernath, *J. Chem. Phys.*, 1993, **99**, 8379.
- J. P. Towle, D.Phil. Thesis, Oxford University, 1992.
- J. M. Brown and A. D. Fackerell, *Phys. Scr.*, 1982, **25**, 351.
- D. H. Rank, U. Fink and T. A. Wiggins, *J. Mol. Spectrosc.*, 1965, **18**, 170.
- F. D. Wayne and H. E. Radford, *Mol. Phys.*, 1976, **32**, 1407.
- C. R. Brazier, R. S. Ram and P. F. Bernath, *J. Mol. Spectrosc.*, 1986, **120**, 381.
- R. S. Ram and P. F. Bernath, *J. Mol. Spectrosc.*, 1987, **122**, 275.
- M. Goto and S. Saito, *Chem. Phys. Lett.*, 1993, **211**, 443.
- V. Stackmann, K. Lipus and W. Urban, *Mol. Phys.*, 1993, **80**, 635.
- A. M. R. P. Bopegedera, C. R. Brazier and P. F. Bernath, *Chem. Phys. Lett.*, 1989, **162**, 301.
- C. A. Coulson, *Valence*, Oxford University Press, London, 1961.
- J. M. Brown, E. A. Colbourn, J. K. G. Watson and F. D. Wayne, *J. Mol. Spectrosc.*, 1979, **74**, 294.